Stability Analysis of Perforated Plate Type Single Stage Suspension Fluidized Bed Without Downcomer

Wei-Ming Lu[†], Sheau-Pyng Ju, Kuo-Lun Tung and Yu-Chang Lu

Department of Chemical Engineering, National Taiwan University, Taipei 106, Taiwan

Abstract–The stability of operation of a perforated plate type suspension bed without downcomer was analyzed experimentally and numerically. The effects of the feed rate, the gas flowrate and the opening ratio and hole diameter of the perforated plates on the operating stability of the fluidized bed were examined. A full three-dimensional discrete particle simulation method proposed by Tsuji [1993] was performed to study the formation of a stable suspension fluidized bed. The course and behavior of particles that formed a dense and stable fluidized bed are discussed. Both the experimental and simulation results of this study show that the process of forming a suspension bed can be categorized into (i) an induced stage, (ii) a growing stage, and (iii) a stable stage. The velocity of gas through the orifice directly controls the formation of the bed while the solid flow rate over a considerable range maintains a balanced hold-up in the suspension bed system without downcomers. The existence of a multiplicity of steady states corresponding to different gas flow rates, for the same feed rate and perforated plate type, was observed. Results show that the design of the plate, the particle feed rate and the gas velocity distribution through the hole affect the stability of the fluidized bed. The simulated results agree qualitatively well with experimental observations.

Key words: Fluidization, Suspension Bed, Stability, Discrete Element Method, Computer Simulation

INTRODUCTION

A fluidized bed offers many advantages, such as a higher transfer coefficient, ideal complete mixing which gives a uniform temperature and concentration distribution throughout the system, and fluid-like handling of solid particles. In order to continuously operate a vertical type fluidized bed system, two methods can be considered: (i) particles passing through downcomers or overflow standpipes, and (ii) particles passing through perforated plates. The major difference between an ordinary fluidized bed with downcomers and a suspension bed on a perforated plate is in the design of the perforated plates. In the former case, a perforated plate with a very small opening ratio rectifies the fluid, and the particles leave the system to the outlet through a downcomer. In the latter case, the opening ratio of the perforated plate is in the range of 25-45%, and the hole diameter is usually 3-10 times of d_p. Thus, the particles flow to the outlet by leaking through these orifices. In this system, perforated plates act both as gas distributors and as stage separators, thus eliminating the need for overflow pipes and downcomers. As compared to the ordinary fluidized bed with downcomers, a perforated plate type suspension bed offers no risk of clogging, low installation cost, low pressure drop, high contact efficiency and good thermal efficiency [Gauthier and Flamant, 1991; Kannan et al., 1994].

A perforated plate type suspension bed without downcomers was first proposed by Toei and Akao in 1957 [Toei and Akao, 1957]. These systems were mainly used as continuous reactors,

dryers or adsorbers [Lu, 1959; Overcashier et al., 1959; Wolf and Resnick, 1963; Toei and Akao, 1968; Papadatos et al., 1975]. Most of the research efforts from late 50s to 70s focused on the hold-up and residence time distribution of particles [Wolf and Resnick, 1963; Raghuraman and Varma, 1973a, b, 1975; Papadatos et al., 1975; Varma, 1975; Krishnaiah and Varma, 1982; Pillay and Varma, 1983]. Bergougnou et al. studied the rate of grid leakage in the system and observed that (i) in the dilute phase regime with simultaneous flow of gas and particles through all the holes, gas passes through the central part of the hole and the particles leak at the periphery; (ii) in the dense phase regime, particles leak through a few holes, and gas flows through the others [Servient et al., 1970, 1972; Briens et al., 1978; Guigon et al., 1978; Briens and Bergougnou, 1984, 1985]. However, few have discussed how the bed is formed and how the design and operation variables affect the stability of the bed [Tanaka et al., 1979; Lu and Chin, 1988]. The design and operation of a multistage perforated plate type fluidized bed strongly depend on the characteristics of the particles, such as the particle size, particle size distribution, shape, and density, and on the feed rate of the particles. It is very time-consuming to use the experimental approach to determine the operation conditions of a perforated plate type fluidized bed. Accordingly, the numerical approach proposed by Tsuji [Tsuji et al., 1992, 1993; Tsuji, 1993], which has become recently quite popular in particle technology, provides a powerful tool for investigating the phenomena involved in such a bed.

In this study, a Lagrangian type numerical simulation in a perforated plate type fluidized bed without downcomers was performed. The motion of all the particles in the bed was calculated three-dimensionally by modeling the contact forces with

[†]To whom correspondence should be addressed.
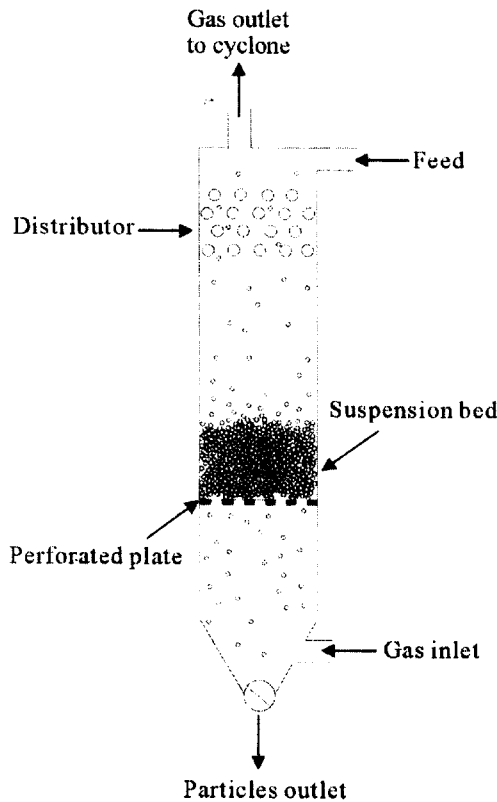E-mail: wmlu@ccms.ntu.edu.tw

Fig. 1. A schematic diagram of a perforated plate type suspension bed system without downcomers.

DEM [Cundall and Strack, 1979]. In order to reduce the computational load, the fluid flow is treated using a simplified approach. Results obtained from experimental observation of the formation of the suspension bed on the perforated plate of the system and analysis of how the operation variables affected the stability of the single stage fluidized bed of this type will be presented.

MODELING OF THE SYSTEM

1. Perforated Plate Type Suspension Bed System

The perforated plate type suspension bed system, shown in Fig. 1, consists of a thin perforated plate in a column without downcomers similar to a perforated-plate distillation column. The dense solid suspension forms on the perforated plate. Particles are fed continuously from the top of the column, and the gas is blown from the bottom. Since there is no downcomer on the perforated plate, the particles fall down to the outlet through the holes, whose diameter is several times that of particles.

2. Simulation Model

In this study, a full three-dimensional discrete particle simulation method was used to analyze the stability of operation of the perforated plate type fluidized bed. The following assumptions were adopted for modeling:

(1) Particles are spherical in shape and uniform in diameter.

(2) The forces acting on one particle in contact with another particle or a wall were modeled using the DEM model using
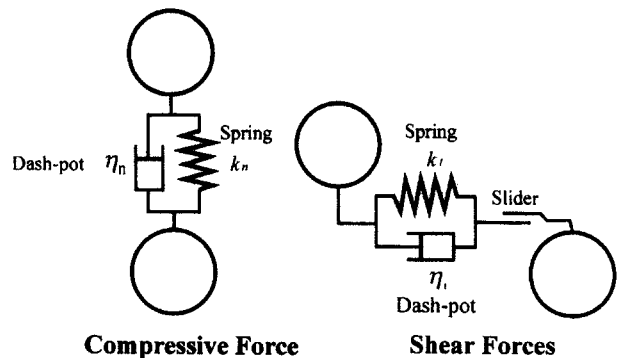

Fig. 2. Cundall model of contact forces.

springs, dash-pots and a friction slider as shown in Fig. 2, following Cundall and Strack [Cundall and Strack, 1979].

(3) Particles are generated from the top of the column and gas is blown from the bottom of the column uniformly.

2-1. Calculation of Particle Motion

Based on the above assumptions, Newton's second law of motion can be used to describe the motion of an individual particle. Thus, the equations governing the translational and rotational motions of particle i at any time t are:

$$m_i \frac{d\mathbf{v}_i}{dt} = \sum \mathbf{F}_i = \mathbf{F}_{f,i} + \sum_{j=1}^{k_i} \mathbf{F}_{c,ij} + \mathbf{F}_{g,i}, \text{ and} \quad (1)$$

$$I_i \frac{d\omega_i}{dt} = \sum_{j=1}^{k_i} \mathbf{T}_{ij}, \quad (2)$$

where m_i and $I_i (=2/5 m_i r_i^2)$ are the mass and the moment of inertia of particle i, respectively, $\mathbf{v}_i$ and ω_i are the velocity and the angular velocity of particle i, respectively, and k_i is the number of particles in contact with this particle i. The forces involved are the fluid drag force, $\mathbf{F}_{f,i}$, the inter-particle forces between particles i and j, $\mathbf{F}_{c,ij}$, and the gravitational force, $\mathbf{F}_{g,i}$. The inter-particle forces will generate a torque, $\mathbf{T}_{ij}$, causing particle i to rotate. For a spherical particle i of radius r_i, $\mathbf{T}_{ij}$ is given by $\mathbf{T}_{ij} = \mathbf{r}_i \times \mathbf{F}_{c,ij}$, where $\mathbf{r}_i$ is a vector running from the mass center of particle i to the contact point with a magnitude of r_i.

The renewal velocity, angular velocity and position of particle i after the time step Δt can be calculated explicitly:

$$\mathbf{v}_i = \mathbf{v}_{i,0} + \frac{\sum \mathbf{F}_i}{m_i} \Delta t, \quad (3)$$

$$\omega_i = \omega_{i,0} + \frac{\sum_{j=1}^{k_i} \mathbf{T}_{ij}}{I_i} \Delta t, \quad (4)$$

$$\delta_i = \delta_{i,0} + \mathbf{v}_i \Delta t, \quad (5)$$

respectively, where subscript 0 denotes the initial value.

2-2. Calculation of Fluid Motion

In a fluidized bed, the presence of particles will disturb the flow of gas. It is difficult even for a supercomputer to directly calculate the instantaneous variation of the local values of the gas velocity and pressure. Therefore, it is reasonable to solve this problem using the local average technique proposed by

Anderson and Jackson [Anderson and Jackson, 1967]. In this study, the flow field of the fluid flow through the perforated plate was calculated first using the SIMPLE algorithm and a control-volume difference technique [Patankar, 1980]. After the particles were fed from the top of the column, the fluid motion was solved simultaneously with the motion of the particles using the local average technique. According to this local average technique, the equation of continuity and the equation of motion are expressed in terms of the local mean variables over the control volume as

$$\frac{\partial \varepsilon}{\partial t} + \Delta \cdot (\varepsilon \mathbf{u}) = 0, \tag{6}$$

$$\frac{\partial (\varepsilon \mathbf{u})}{\partial t} + \Delta \cdot (\varepsilon \mathbf{u} \mathbf{u}) = -\frac{\varepsilon}{\rho_f} \Delta p - \mathbf{F}. \tag{7}$$

All the quantities, such as the particle velocity and pressure, are averaged in the control-volume using a weight function. The term $\mathbf{F}$ represents the interaction between the particles and the fluid, and is given by [Prichett et al., 1978]

$$\mathbf{F} = \frac{\psi}{\rho_f} (\mathbf{u} - \mathbf{v}). \tag{8}$$

The above coefficient ψ is a function of the bed porosity and can be deduced from the Ergun equation as follows:

$$\psi = \begin{cases} \dfrac{1-\varepsilon}{d_p \varepsilon^2} \left[150 \dfrac{\mu(1-\varepsilon)}{d_p} + 1.75 \rho_f \varepsilon |\mathbf{u} - \mathbf{v}| \right], & \text{for } \varepsilon \leq 0.8 \\[12pt] \dfrac{3}{4} C_D \dfrac{|\mathbf{u} - \mathbf{v}| \rho_f (1-\varepsilon) \varepsilon^{-2.7}}{d_p} & \text{for } \varepsilon > 0.8 \end{cases} \tag{9}$$

$$C_D = \begin{cases} \dfrac{24}{Re_p}(1 + 0.15 Re_p^{0.687}), & \text{for } Re < 1,000 \\[8pt] 0.43 & \text{for } Re > 1,000 \end{cases} \tag{10}$$

$$Re_p = \frac{\rho_f \varepsilon d_p}{\mu} |\mathbf{u} - \mathbf{v}|. \tag{11}$$

2-3. Modeling of Contact Forces

The forces acting on a particle in contact with another particle or a wall can be modeled using the DEM model using springs, dash-pots and a friction slider as shown in Fig. 2, following Cundall and Strack [Cundall and Strack, 1979]. The model shown in Fig. 2 is the same as the Voigt model used in the field of rheology. The effects of these mechanical elements on particle contact appear through the following parameters:

the stiffness of the spring, k, the damping coefficient of viscous dissipation, η, and the friction coefficient, f. When particle i is in contact with particle j, the linear normal and tangential components of the contact force acting on particle i are given by the sum of the forces acting on the spring and the dash-pot as

$$\mathbf{F}_{ct,ij} = [-k_{n,i} - \delta_{n,ij} - \eta_{n,i}(\mathbf{v}_i - \mathbf{v}_j) \cdot \mathbf{n}_n] \mathbf{n}_n \tag{12}$$

and

$$\mathbf{F}_{ct,ij} = -(k_{t,i} \delta_{t,ij}) \mathbf{n}_t - \eta_{t,i}[(\mathbf{v}_i - \mathbf{v}_j) \cdot \mathbf{n}_t + (\omega_i \times \mathbf{r}_i - \omega_j \times \mathbf{r}_j)] \mathbf{n}_t, \tag{13}$$

respectively, where $k_{n,i}$, $\eta_{n,i}$ and $\delta_{n,ij}$, and $k_{t,i}$, $\eta_{t,i}$ and $\delta_{t,ij}$ are, respectively, the stiffness of the spring, the viscous contact damping coefficient and the displacement of particle i in the normal and tangential directions; $\mathbf{n}_n$ and $\mathbf{n}_t$ are the unit vectors along the normal and tangential directions, respectively. When particle j is replaced by the wall, $|\mathbf{v}_j| = |\omega_j| = 0$. If $|\mathbf{F}_{ct,ij}| > f_{ij} |\mathbf{F}_{cn,ij}|$, then sliding occurs, and the magnitude of the tangential force is given by the Coulomb friction law as

$$\mathbf{F}_{ct,ij} = -f_{ij} |\mathbf{F}_{cn,ij}| \mathbf{n}_n \tag{14}$$

instead of Eq. (12). The displacement is given by $\delta_{t,ij} = \mathbf{F}_{ct,ij}/k_t$.

2-4. Simulation Procedures

The simulation procedures used in this study are shown in Fig. 3, where the modeling of the solid flow using DEM is conducted at the individual particle level while the gas flow by CFD is conducted at the computational cell level. This simulation procedure is both stochastic and deterministic. The stochastic nature of this approach derives directly from the randomness at the feeding inlet of the positions of the generated particles. However, once we know the initial position of a given particle along with the flow field around the perforated plate as well as the operating force, its trajectory can be identified. The instantaneous number of generated particles is calculated using a particle balance for a set feed rate, and the initial conditions of the particles are determined using a numerical generator with a random distribution function. During the simulation, the magnitude of each time increment, Δt, must be small enough for the variations of external forces in each time interval to be neglected. Therefore, $\Delta t = 1 \times 10^{-6}$ s was chosen in this study. The trajectory of each particle is predicted by the equation of motion of the particle using the Lagrangian approach. If the instantaneous linear and angular acceleration of a particle have been obtained, Newton's second law of motion can be used to
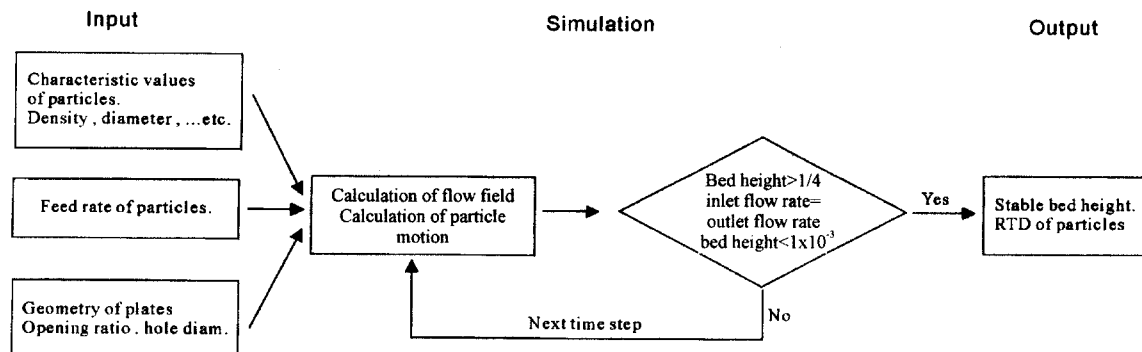

Fig. 3. A flow diagram of the simulation procedure.

update the motion of the particle. The renewal linear velocity, angular velocity and position vector can be obtained using Eqs. (3), (4) and (5), respectively. In a fluidized bed, the presence of particles will disturb the flow of gas. It is difficult even for a supercomputer to directly calculate the instantaneous variation of the local values of the gas velocity and pressure. However, the time scale for particle motion is much smaller than that of fluid motion; therefore, the flow field can be calculated based on the local average technique using Eqs. (6) and (7) at each time increment. The simulation time step is repeated until the forming bed is regarded to be stable. In this study, the criteria for a stable bed are the following: the particles flow rate at the inlet matches that at the outlet of the column, and the net accumulation of particles on the bed is equal to zero. As the simulation proceeded, the time courses of the variation of the bed porosity, RTD of particles, pressure drop, and hold-up were recorded.
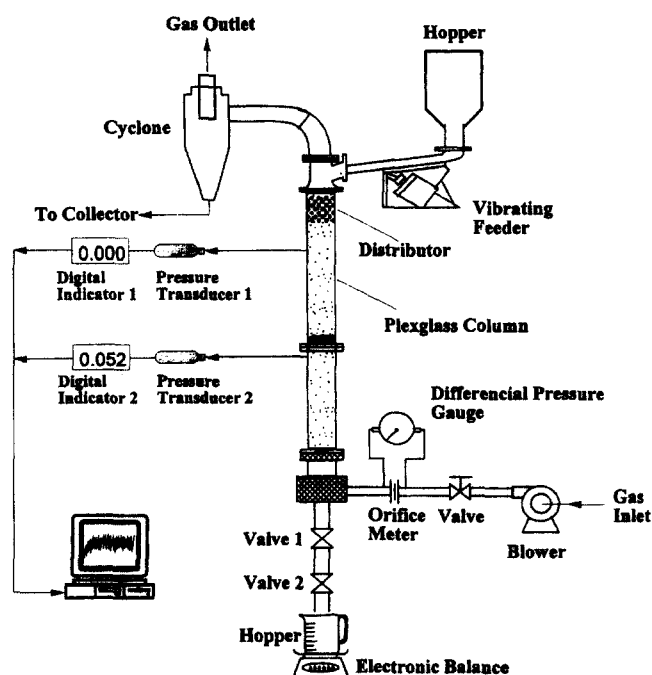

Fig. 4. A schematic diagram of the experimental apparatus.

Table 1. Numerical values of the parameters and physical properties of the particles and fluid

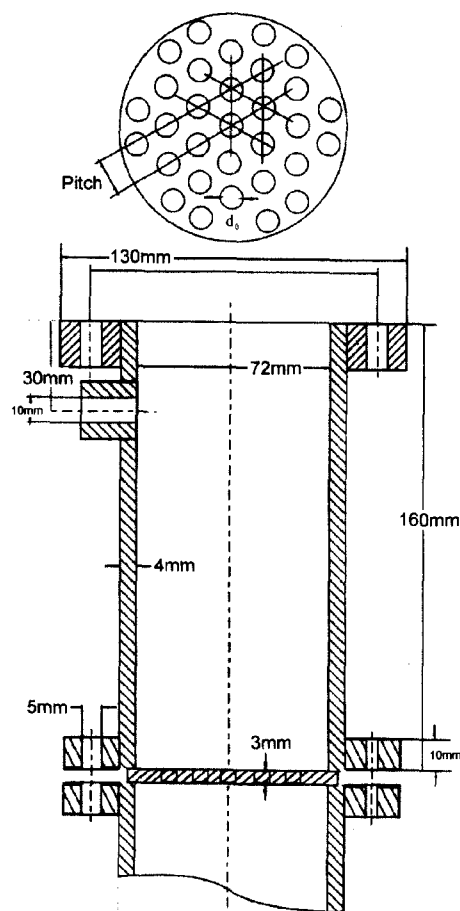| Parameters and variables	Numerical values
Stiffness of spring k [N/m]	800
Coeff. of friction f [-]	0.3
Damping coeff. η [-]	0.15
Particle diameter d_p [mm]	2.0
Particle density ρ_s [kg/m³]	1050.0
Feed rate F [kg/ m²s]	0.05-0.13
Gas density ρ_f [kg/m³]	1.20
Gas viscosity μ [kg/m s]	1.80×10^{-5}
Gas flow rate U_o [m/s]	1.0-7.0
Perforated hole dia. d_h [mm]	5.0, 7.0
Perforated plate opening ratio [-]	26.8, 33.2

Fig. 5. A detailed diagram of the fluidized column and perforated plate.
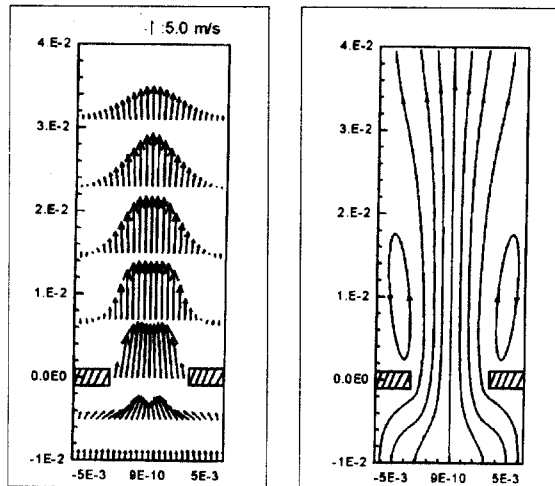
EXPERIMENTAL

Experiments were carried out in a single stage transparent Plexiglas column with an inside diameter of 0.07 m as shown in Fig. 4. Triangular pitch perforated plates with different hole diameters, d_h=7 mm and 5 mm, were prepared for experiments with different operating conditions (as shown in Fig. 5). Polystyrene beads were fed into the system through a constant rate feeder that was a combination of an orifice hopper and a vibrating feeder. Table 1 shows the physical properties of the materials used in this study. Hold-up on the plate was determined from the net pressure drop of the bed while total hold up was measured directly [Tanaka et al., 1979] after the inlet was closed while a stream of solid flow continued. The dynamic pressure drop across the suspension bed was measured using a differential pressure transducer that produced an output voltage proportional to the pressure fluctuation. The voltage-time signals were converted to digital signals by an AD/DA converter and recorded in a PC.
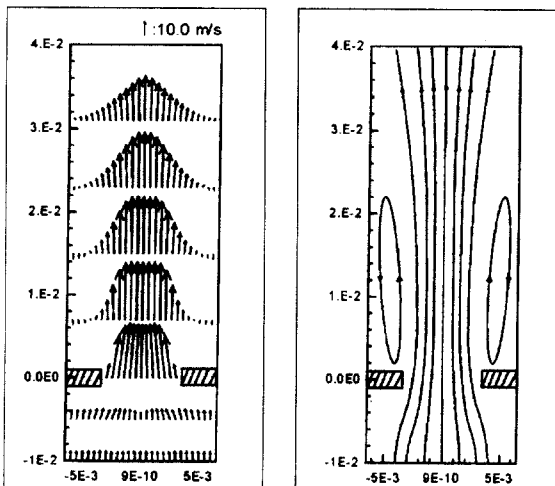
RESULTS AND DISCUSSION

1. Flow Pattern in a Perforated Plate Type Fluidized Bed

The calculation conditions are summarized in Table 1. Fig. 6 shows the axis-symmetric patterns of the velocity vectors and

(a) $U_O = 3.33$ m/s

(b) $U_O = 6.66$ m/s

Fig. 6. Velocity vectors and streamlines of fluid flow through a hole with diameter=7 mm.

the streamlines of the fluid flow through a perforated plate with a hole diameter d_h=7.0 mm and an opening ratio=26%. The periodical boundary condition was employed in the calculation of the fluid flow through the perforated hole. A pair of recirculating regions formed near the upper part of the perforated hole. The central tip velocity was about six times greater than the value of the superficial velocity. Fig. 7 illustrates the combined
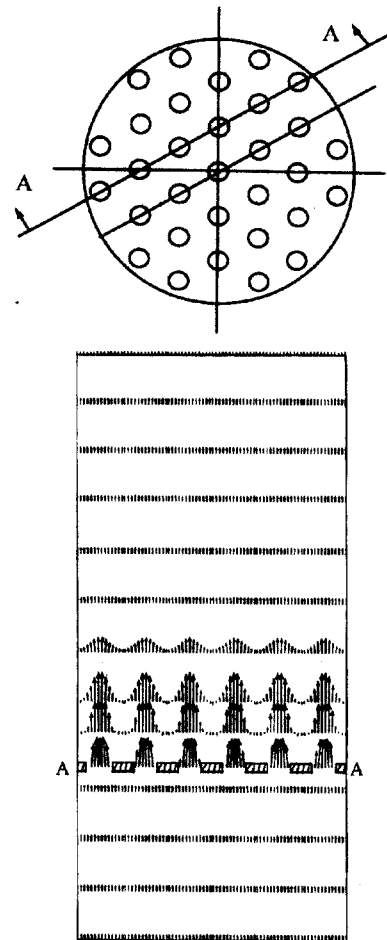

Fig. 7. Flow pattern in a single stage perforated plate type fluidized bed (A-A section).

velocity vector of the flow pattern in a single stage perforated plate type fluidized bed across the A-A section. This figure shows that most of the disturbance of the flow field occurred near the orifice plate. The velocity profile passing through the hole significantly affected the particle motion above the orifice. Microscopic observation of the simulated results of particle motion near the orifices shows that particles ascended in the center region where the effect of the discharge gas appeared to be dominant and descended in the void free region before entering the central region again as shown in Fig. 8.

2. Formation and Stability of a Single Stage Suspension Bed
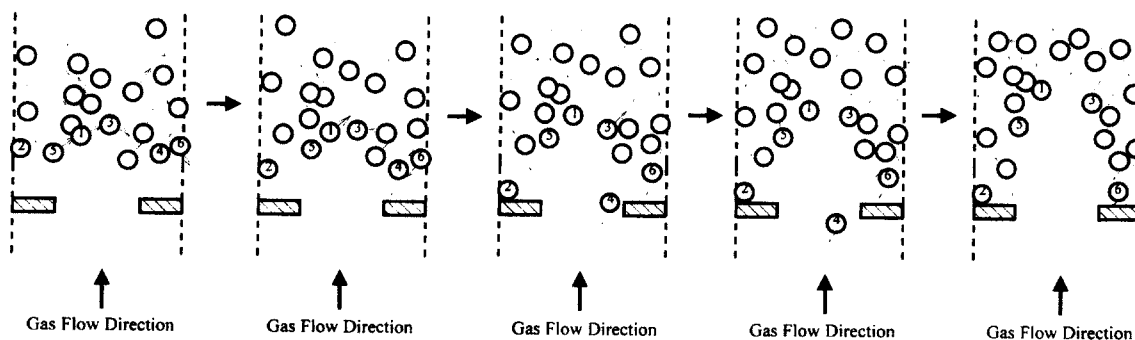

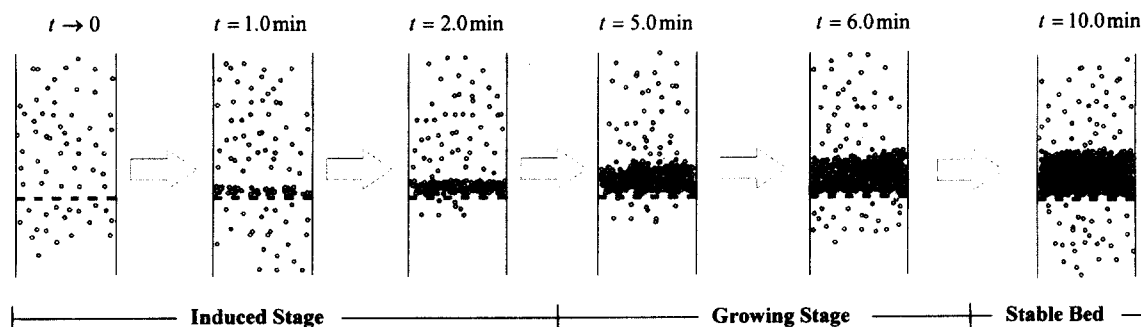**Fig. 8. Simulated results of particle motion above the orifice.**

Fig. 9. Simulated results of transient course formation of a single stage suspension bed.

The simulated results shown in Fig. 9 show how a suspension bed develops at a fixed particle feed rate. The solid leakage rate first decreases abruptly first and then recovers to a rate

(a) Experimental Result

(b) Simulated Result

Fig. 10. Transient variation of the pressure fluctuation across the bed during suspension bed formation.

equal to the feed rate during the course of development. Fig. 10 depicts the transient variations of the pressure fluctuation across the bed. The pressure drop, Δp, through the suspension bed is also a measure of the hold-up of the particles. The hold-up of the particles on the plate can be determined from the net pressure drop across the bed and should satisfy the relationship $W_H \cong \Delta p(g_c/g)$ [Toei and Akao, 1968]. A comparison of the experimental and simulated pressure fluctuation courses is shown in Figs. 10(a) and (b). It shows that agreement is good for the frequency but not very good for the amplitude of fluctuation. The minimum fluid velocity which is needed to suspend the particle above the orifice may be defined as the minimum suspension velocity, U_m, and the transient course shown in Fig. 9 can be divided into three stages: (1) an induced stage, (2) a growing stage, and (3) a stable stage.
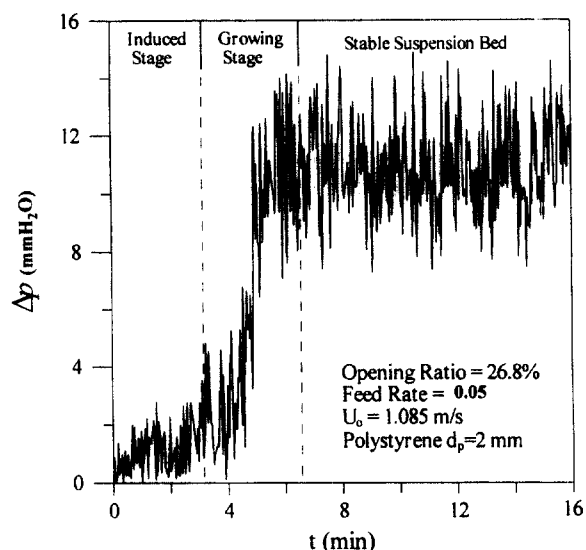
(1) Induced stage: For a given particle feed rate, and as the gas flow rate increases to 50-60% of the terminal velocity of the average particle, the rate of leakage of solid particles through the orifices begins to decrease sharply because the particles start to suspend on the plate, forming a very lean bed. This lean bed intercepts more particles until particles cover almost the whole orifice. At this stage, the leakage rate reaches a minimum, and leads to a rapid increase in the hold-up of the particles on the plate.

(2) Growing stage: As the hold-up of the particles continuously increases and a dense bed forms, a spout bed-like phenomenon can be observed around each orifice. Leakage of particles takes place via a dumping or weeping mechanism. Switch phenomena are also observed among the orifices. At this stage, the feed rate is still higher than the discharge rate; thus, the hold-up of the bed will increase continuously during this stage.
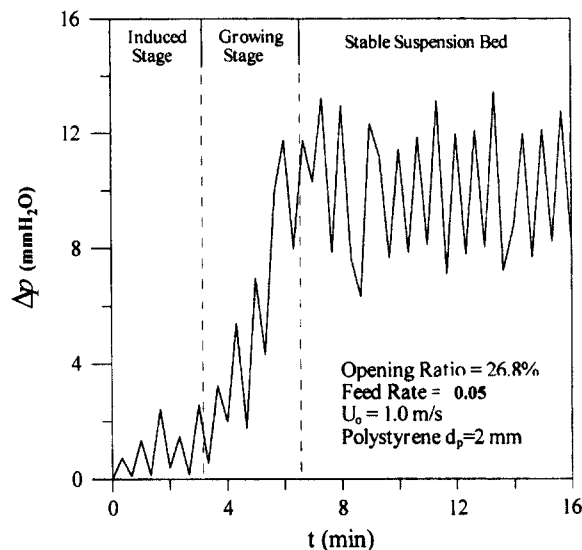
(3) Stable stage: As the leakage rate reaches the level of the feed rate, the bed height and the hold-up of particles reaches steady state. This stage may be called the stable stage. Since the suspension bed is very sensitive to any change in the gas flow rate, feed rate or other operational conditions, even a small change in the gas flow rate or solid feed rate will result in a continuous increase or decrease of the solid hold up. In this case, the bed will reach another stable height corresponding to the new gas flow rate or feed rate.

3. Characteristics of a Single Stage Suspension Bed

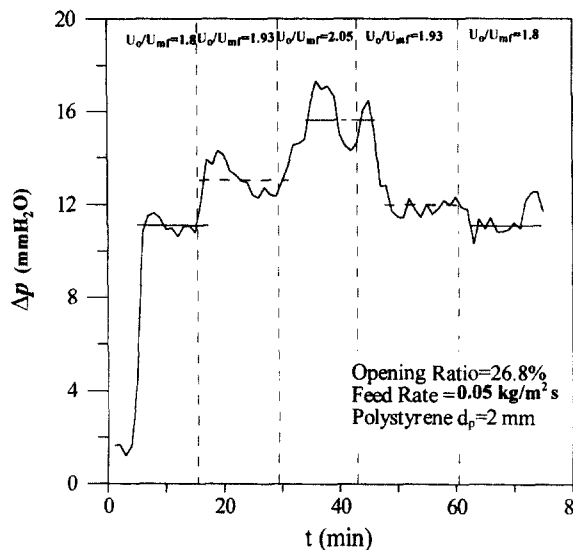Fig. 11 shows a multiplicity of steady states corresponding

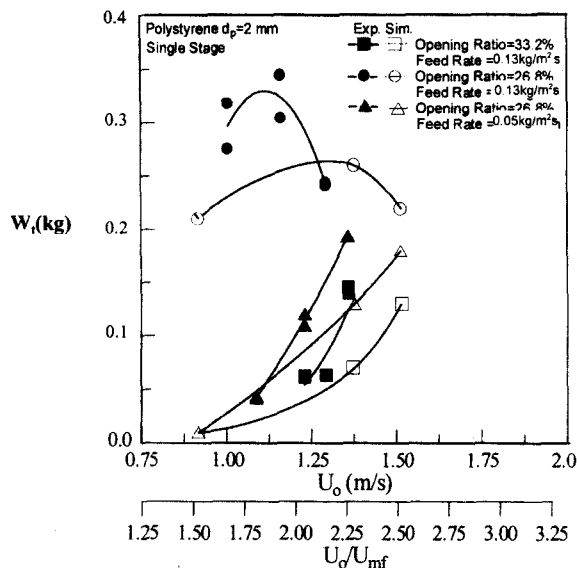Fig. 11. Experimental results for multiple steady states.

Fig. 12. Hold-up vs. U_o in a single stage bed under different feed rates.

to different gas flow rates, for the same feed rate and perforated plate type. A hysteresis phenomenon in the pressure fluctuation was observed at a higher gas flow rate. This was mainly due to the change of the path of bed formation. The performance of a single stage suspension bed was studied to obtain a basis for analysis of the stability of a multistage suspension bed. Fig. 12 shows hold-up of the solid vs. the orifice velocity for various design plates as well as two different feed rates. The plate with the small opening ratio holds more suspended particles and builds a suspension bed at a lower minimum suspension velocity. The plate with the large opening ratio can operate over a wide range of operational variables, including the gas flow, feed rate etc. The results also show that the high rate of descent causes more collisions among the particles in the bed. This collision phenomenon slows down the rate of descent, which results in a higher solid hold-up on the plates. However, it is remarkable

to see that in the condition of the opening ratio 26.8% and higher feed rate 0.13 kg/m²s, both the experimental and simulated results show a convex tendency for the solid hold-up vs. gas flow rate. The reason is that for small opening ratio of perforated plate, the increase of gas flow rate will result in violence of the bed. Under this circumstance, part of the bed fluidized particularly violently and this localized violence was seen to move round the plate with time. Thus it looked as if the fluidized was circulating about the plate and some of the bubbles formed on the plate. The circulation of the bed and formation of bubbles will cause leakage of particles through a few holes, and gas will flow through the other holes. This phenomenon somewhat is very similar to "channeling" in fluid flow through particulate bed. The calculation results agree qualitatively well with the observations made in the experiments.

CONCLUSION

Analysis of the formation and stability of a perforated plate type suspension bed without downcomers has been presented. Both the experimental and simulation results obtained in this study show that the formation of a suspension bed can be categorized into (1) an induced stage, (2) a growing stage, and (3) a stable stage. There exist three types of suspension beds: lean beds, stable beds and unstable or accumulated beds. The velocity of the gas through the orifice directly controls the formation of the bed, while the solid flow rate over a considerable range maintains a balanced hold-up in a suspension bed system without downcomers. A multiplicity of steady states corresponding to different gas flow rates, for the same feed rate and perforated plate type, was observed. Results show that the design of the plate, the particle feed rate, and gas velocity profile through the hole affect the stability of the fluidized bed. The simulated results agree qualitatively well with observations made in the experiments.

NOMENCLATURE

C_D : rag coefficient [-]
d_h : perforated hole diameter [m]
d_p : particle diameter [m]
f : frictional coefficient [-]
F : feed rate of particles [kg/m²s]
F : sum of forces acting on a particle [N]
F_c : contact force [N]
F_d : fluid drag force [N]
F_g : gravitational force [N]
g : acceleration due to gravity [m/s²]
g_c : gravitational conversion factor [kg m/N s²]
I : inertial moment of a particle [kg/m²]
k : stiffness of the spring [N/m]

k_i : number of particles in contact with a particle i [-]
m : particle mass [kg]
n : unit vector [-]
p : pressure [Pa]
Δp : pressure drop across the bed [Pa]
Re_p : particle Reynolds number defined by Eq. (11) [-]
r : particle radius [m]
T : torque [Nm]
t : time [s]
Δt : time increment [s]
u : fluid velocity vector [m/s]
U_m : minimum suspension velocity [m/s]
U_0 : superficial gas velocity [m/s]
v : particle velocity vector [m/s]
W_H : hold-up of particles [kg/m^2]
W_t : total weight of particles on the bed [kg]

Greek Letters

δ : particle displacement vector [m]
ε : void fraction (porosity) [-]
η : damping coefficient [kg/s]
μ : kinetic viscosity of gas [kg/m s]
ρ_f : fluid density [kg/m^3]
ρ_p : particle density [kg/m^3]
ω : particle angular velocity vector [1/s]

Subscripts

0 : initial value
i : particle i
ij : between particles i and j
j : particle j
n : normal component
p : particle phase
t : tangential component

REFERENCES

Anderson, T. B. and Jackson, R., "A Fluid Mechanical Description of Fluidized Beds," I&EC Fund., 6, 527 (1967).

Briens, C. L. and Bergougnoun, M. A., "Grid Leakage (Weeping and Dumping) in a Pilot Size Gas Fluidized Bed," Can. J. Chem. Eng., 62, 455 (1984).

Briens, C. L. and Bergougnou, M. A., "Further Work on Grid Leakage in a Pilot-plant Size Gas-Fluidized Bed," Powder Technol., 42, 255 (1985).

Cundall, P. A. and Strack, O. D. L., "A Discrete Numerical Model for Granular Assemblies," Géotechnique, 29, 47 (1979).

Gauthier, D. and Flamant, G., "Residence Time Distribution in a Series of Three Tanks with Bypass and Back-Mixing: Application to Multistage Fluidized-Bed," Chem. Eng. Comm., 100, 77 (1991).

Guigon, P., Large, J. F., Bergougnou, M. A. and Baker, C. G. J., "Particle Interchange Gas Fluidized Beds," Proceedings of the 2nd Engineering Foundation Conf. on Fluidization, Cambridge Univ. press, 134 (1978).

Kannan, C. S., Rao, S. S. and Varma, Y. B. G., "A Study of Stable of Operation in Multistage Fluidized Beds," Powder Technol., 78, 203 (1994).

Lu, W. M., "Fluidized-bed Dryer," Taiwan Engineering, 12, 39 (1959).

Lu, W. M. and Chin, Y. S., "Characteristics of Multistage Perforated Plate Type Fluidized Bed without Downcomer," Proc. 1st ASCON FBR, Tokyo, Japan, 95 (1988).

Overcashier, R. H., Todd, D. B. and Olney, R. B., "Some Effects of Baffles on a Fluidized System," AIChE J., 5, 54 (1959).

Papadatos, K., Svrcek, W. Y. and Bergougnoun, M. A., "Holdup Dynamics of a Single Stage Gas-Solid Fluidized Bed Adsorber," Can. J. Chem. Eng., 53, 686 (1975).

Patankar, S. V., "Numerical Heat Transfer and Fluid Flow," Hemisphere, New York (1980).

Pillay, P. S. and Varma, Y. B. G., "Pressure Drop and Solids Holding Time in Multistage Fluidization," Powder Technol., 35, 223 (1983).

Raghuraman, J. and Varma, Y. B. G., "Residence Time Distribution of Solids in Multistage Fluidized Beds," Chem. Eng. Sci., 28, 305 (1973a).

Raghuraman, J. and Varma, Y. B. G., "A Model for Residence Time Distribution in Multistage Systems with Cross-Flow be-tween Active and Dead Regions," Chem. Eng. Sci., 28, 585 (1973b).

Raghuraman, J. and Varma, Y. B. G., "An Experimental Investigation of the Residence Time Distribution of Solids in Multistage Fluidization," Chem. Eng. Sci., 30, 145 (1975).

Serviant, G. A., Bergougnou, M. A., Baker, C. G. J. and Bulani, W., "Grid Leakage in Fluidized Beds," Can. J. Chem. Eng., 48, 496 (1970).

Serviant, G. A., Bergougnou, M. A. and Baker, C. G. J., "Further Studies on Grid Leakage in Gas Fluidized Beds," Can. J. Chem. Eng., 50, 690 (1972).

Tanaka, I., Ishikura, T., Uchiyama, A. and Shinohara, H., "Fluid Characteristics of Continous Multiperforated Plate Stage Fluidized Beds without Downcomer," Kagaku Kogaku Ronbunshiu, 5, 397 (1979).

Toei, R. and Akao, T., "Roasting of Wheatgrain by Multistage Fluidized Bed," private communication (1957).

Toei, R. and Akao, T., "Multistage Fluidized Bed Apparatus with Perforated Plates," IChemE Symp. Series, 30, 34 (1968).

Tsuji, Y., Tanaka, T. and Ishida, T., "Lagrangian Numerical Simulation of Plug Flow of Cohesionless Particles in a Horizontal Pipe," Powder Technol., 71, 239 (1992).

Tsuji, Y., Kawaguchi, T. and Ishida, T., "Discrete Particle Simulation of Two-Dimensional Fluidized Bed," Powder Technol., 77, 79 (1993).

Tsuji, Y., "Discrete Particle Simulation of Gas-Solid Flows-From Dilute to Dense Flows," KONA, 11, 57 (1993).

Varma, Y. B. G., "Pressure Drop of the Fluid and the Flow Patterns of the Phases in Multistage Fluidization," Powder Technol., 12, 167 (1975).

Wolf, D. and Renick, E., "Experimental Study of Residence Time Distribution in a Multistage Fluidized Bed," I&EC Fund., 4, 287 (1963).